IEEE Access
Multidisciplinary | Rapid Review | Open Access Journal

Received January 2, 2020, accepted February 20, 2020, date of publication February 27, 2020, date of current version March 12, 2020.

*Digital Object Identifier 10.1109/ACCESS.2020.2976516*

# Temperature Sensing Characteristics and Long Term Stability of Power LEDs Used for Voltage vs. Junction Temperature Measurements and Related Procedure

**FRANCESCO G. DELLA CORTE, (Senior Member, IEEE), GIOVANNI PANGALLO, RICCARDO CAROTENUTO, (Senior Member, IEEE), DEMETRIO IERO, GIUSEPPE MARRA, MASSIMO MERENDA, (Member, IEEE), AND SANDRO RAO, (Member, IEEE)**

Dipartimento di Ingegneria dell'Informazione, delle Infrastrutture e dell'Energia Sostenibile (DIIES), Mediterranea University of Reggio Calabria, 89122 Reggio Calabria, Italy

Corresponding author: Francesco G. Della Corte (francesco.dellacorte@unirc.it)

**ABSTRACT** A detailed study about the direct measurement of junction temperature $T_J$ of off-the-shelf power light emitting diodes (LED) is presented. The linear dependence on temperature of the voltage drop across the device terminals at a constant current is in particular exploited and fully characterized, in the temperature range from $T = 35$ °C to 135 °C, with tests repeated at one thousand different probe currents. The accurate experimental data, obtained on several LED samples bearing two different part numbers, are reported, showing that they exhibit a high degree of linearity in wide current ranges, a circumstance that allows for a fast and reliable calibration as sensors. The measurement error is also fully characterized in terms of repeatability and stability over time, with measurements repeated after 600, 900, 1200 and 1800 hours of applied electro-thermal stress, demonstrating that the relevant sensor parameters stabilize after a few hundred hours of operation. A full set of parameters is provided for the two device models, allowing the direct use of each LED for the self-monitoring of the junction temperature and ensure compliance with their safe operating area over time. Moreover, a procedure and a simple circuit for the real time measurement of $T_J$, while the LED is on, are presented. The procedure does not require a stable current source, and relies instead on the application of a sub-threshold current ramp for such a short time that the change in the output light is not perceived by human eyes.

**INDEX TERMS** LED, light emitting diodes, junction temperature, temperature sensors, diode sensors.

## I. INTRODUCTION

The Solid State Lighting (SSL) technology has definitively emerged as the most efficient and long lasting technology for converting electricity into light in almost every application context, from luminaries to flat panel displays, to wide area image projection. In fact, it has brought significant advancements in terms of energy and cost savings. Light emitting diodes (LEDs) are the heart of SSL lighting products and can provide long lifetimes that last well beyond thousands of hours of operation, much longer than most conventional light sources. Moreover, LEDs exhibit the additional advantage that, in most cases, instead of sharply falling to zero, the light intensity output may slowly fade or the color slowly degrade as the end of life is approaching [1]–[5].

It is well known, however, that LED performances, at least in terms of intensity, lifetime and emission spectrum, degrade faster as their operation temperature increases above certain limits [6]–[12], which unfortunately are set well below those of incandescent bulbs and even of fluorescent lamps. These limits can also be easily reached during normal operation because, despite their excellent conversion efficiency, the LEDs heat up quickly due to their very limited active area and consequent high power density. It turns out that high quality solid-state light sources must always adopt more or less complex temperature control strategies, including passive or active cooling methods [13].

The main thermal parameter of an LED is its junction temperature, $T_J$. Many methods have been proposed in the

The associate editor coordinating the review of this manuscript and approving it for publication was Jiajie Fan.

literature for monitoring the junction temperature based on LED electroluminescence [14], Raman spectroscopy [15], [16], light spectrum [17], liquid crystal thermography [18] or on the use of external temperature sensors that allow estimating the LED junction temperature [19], [20]. All these methods [14]–[20] require an additional external sensor for extracting the actual $T_J$.

Normally, $T_J$ is estimated starting from the thermally dissipated power $P_D$ and the thermal resistance $R_\Theta$ of the device, being in fact $T_J = P_D \cdot R_\Theta + T_X$, with $T_X$ the environment temperature [21], [22]. However, knowing $P_D$ and $R_\Theta$ is not straightforward as it may seem, because the former is only a small fraction of the overall electric power dissipated by an LED, with the biggest part converted into light, while measuring the thermal resistance involves complex procedures and its value may change over time and with temperature itself [22].

There are however other ways to monitor an LED $T_J$, consisting of using its own electrical parameters, *e.g.* the reverse saturation current $I_S$ [23] or the forward voltage $V_F$ under a constant current [24]–[27], that are in fact both temperature dependent.

In this work we analyze a large set of experimental data showing that the $V_F$ vs. $T_J$ relationship can be optimized to perform an excellent linearity, allowing to easily and reliably measure the internal device temperature, without involving an external temperature sensor. The technique is developed starting from previous studies carried out on diodes of various types and sizes [28]–[31], and is here shown to be perfectly suitable also for LEDs, and further improved to make the measurement faster and the measuring circuit simpler. It is worth noting that a highly linear dependence in a wide temperature range allows the simplest experimental pre-calibration procedure of the device, which can be in fact carried out at just two temperatures.

Once the LED is calibrated, the procedure adopted hereafter allows to calculate $T_J$ by dropping the standard fixed-current approach [22], [24]–[31], and launching instead a current ramp, within an appropriate range, during which random current-voltage measurements are performed until a measurement at the desired probe current is detected.

The sensor sensitivity, together with the linearity of the output characteristics, are analyzed in a wide range of bias currents and temperatures, from 35 °C to 135 °C. The experimental measurements, repeated on 6+6 devices with two different part number, demonstrate the possibility of implementing the new method for monitoring and controlling the LED junction temperature in order to increase its lifetime and performances.

A microcontroller-based circuit is finally presented performing the measurement procedure at regular intervals. The acquisition lasts less than 10 ms, a short enough time to have no practical effects on the light perceived by the human eye.

The paper is organized as follows. In Section II, the linear dependence between the forward voltage falling on an LED and its junction temperature, the experimental setup and the characterization method are described. Section III reports the experimental results with particular attention to the temperature sensor performance, *i.e.* linearity, sensitivity and temperature error for a single LED.

Afterward, the average characteristic parameters are calculated for each device type, after several operation intervals. In Section IV, an example of a practical circuit for a real-time measurement of the junction temperature of an LED is presented. Finally, conclusions are drawn in Section V.

## II. EXPERIMENTAL SETUP AND CHARACTERIZATION METHOD

As well known, the electrical characteristics of power LEDs are similar to those of all diodes. Every diode, either p-i-n, p-n or Schottky, can be used as a temperature sensor when it is crossed by a known current, $I_F$, kept constant over the whole temperature measuring range [29]–[33]. In fact, a relationship exists in this case between the voltage drop appearing at the junction and $T_J$, allowing an indirect and accurate temperature measurement. To avoid self-heating effects, the sensor must be biased at low currents, which also optimizes power consumption. For accurate measurements, this relationship must be pre-determined experimentally. However, to understand its origin and the key parameters involved, one can recall that, in its simplest formulation, the diode current $I_F$ at a given applied voltage, $V_F$, can be modeled by the following formula:

$$I_F = I_S \left( e^{\frac{q(V_F - R_S I_F)}{\eta k T_A}} - 1 \right), \tag{1}$$

where $\eta$ is the ideality factor, $I_S$ is the saturation current, $R_S$ is a stray series resistance, $q$ is the electron charge, $k$ is the Boltzmann constant and $T_A$ is the device absolute temperature. Note that in (1) $V_F$ is the overall voltage drop externally appearing at the device terminals, while $(V_F - R_S \cdot I_F)$ represents the voltage drop internally appearing at the real device junction. When the diode is forward biased and $q(V_F - R_S \cdot I_F) \gg \eta k T_A$, the relationship between $V_F$ and $T_A$ can be obtained from (1):

$$V_F = \frac{kT_A}{q} \eta ln \left( \frac{I_F}{I_S} \right) + R_S I_F. \tag{2}$$

In (2), $T_A$ explicitly appears as a linear term, but it also implicitly and non-linearly affects $I_S$ and $R_S$, while $\eta = 1$ if the device operates in the diffusion regime. However, it has been demonstrated in many diodes [29]–[31], [34] that an excellent linearity between $V_F$ and $T_A$ can be reached, in a wide temperature range, by properly choosing $I_F$.

In particular, if $R_S$ and $I_F$ are sufficiently small, their product is negligible, and by explicating $I_S$ as [35]:

$$I_S = C T_A^\alpha e^{-\frac{E_g}{kT}}, \tag{3}$$

where $C$ and $\alpha$ are constants, $E_g$ is the extrapolated energy bandgap at 0 K, from (2) we find:

$$V_F = \eta \frac{k}{q} \left[ T_A \left( lnI_F - lnC \right) - \alpha T_A lnT_A + \frac{E_g}{k} \right]. \tag{4}$$

At a fixed $I_F$, and constant $\eta$, $C$ and $\alpha$, the only non-linear term in (4) is $\alpha\ T_A \ln T_A$. However, it can be shown that this term has in fact a high degree of linearity in the temperature range of interest for LEDs, *i.e.* from room temperature to 420 K. It turns out that (4) shows in turn a high degree of linearity with $T_A$ in the same range.

In our study, we focused on two commercial white light power LEDs, denoted hereafter as LED-A [36] and LED-B [37], having respectively a normal operation current of 700 mA at 3.05 V and 1050 mA at 3.02 V. The maximum working temperature is 150 °C for both types.

Firstly, a set of measurements was carried out to identify the most suitable bias current range where these LEDs can work as linear temperature sensors. The used setup was already described in [38]. The tests, made on six devices of each type, consisted in increasing and decreasing the temperature in steps of 10 °C in a thermostatic oven (Fratelli Galli G-2100 [39]) with a regulation accuracy of ±1 °C. A PT100 temperature sensor (with an accuracy of 0.2 °C) was also tightly placed in contact with the printed circuit board (PCB), made of alumina, hosting the devices under test (DUT), in order to monitor their exact temperature inside the oven, which was gradually varied from 25 °C up to 135 °C and *vice versa*. The current-voltage ($I_F$-$V_F$) characteristics were measured with an Agilent 4155C semiconductor parameters analyzer [40], programmed for providing a bias current ($I_F$) gradually rising from 10 $\mu$A up to 10 mA, in steps of 10 $\mu$A. Note that at these low currents the LEDs emit a very weak radiation, or they give no emission at all. At each step, measurements started only after the settling of a stable temperature for several minutes.

The current-voltage-temperature $I_F$-$V_F$-$T$ characteristics were subsequently elaborated and the linear fitting was calculated in order to assess the degree of linearity of the response, the device temperature sensitivity and the root mean square error.

Finally, as better detailed in the next section, the LEDs were driven at a normal operating current and a temperature of 80 °C for 1800 h, and the current-voltage-temperature measurements were repeated to verify the long-term response of the devices.

## III. EXPERIMENTAL RESULTS

### A. VOLTAGE-TEMPERATURE CHARACTERISTICS

The dc bias current, $I_F$, was varied in a range from 10 $\mu$A to 10 mA, in steps of 10 $\mu$A, and the corresponding voltage drop $V_F$ across the LED was measured. Typical $I_F$-$V_F$ characteristics for both LED types are reported in Fig. 1, measured in the temperature range from 25 °C to 135 °C, in steps of 10 °C.

Typical voltage-temperature ($V_F$-$T$) characteristics for both LED types, at several probe currents ($I_F$), are shown in Fig. 2. As expected, at all currents the voltage drop decreases by increasing the temperature. Moreover, in Fig. 2 the linear fittings are also reported, showing that the LED responses have an excellent degree of linearity.

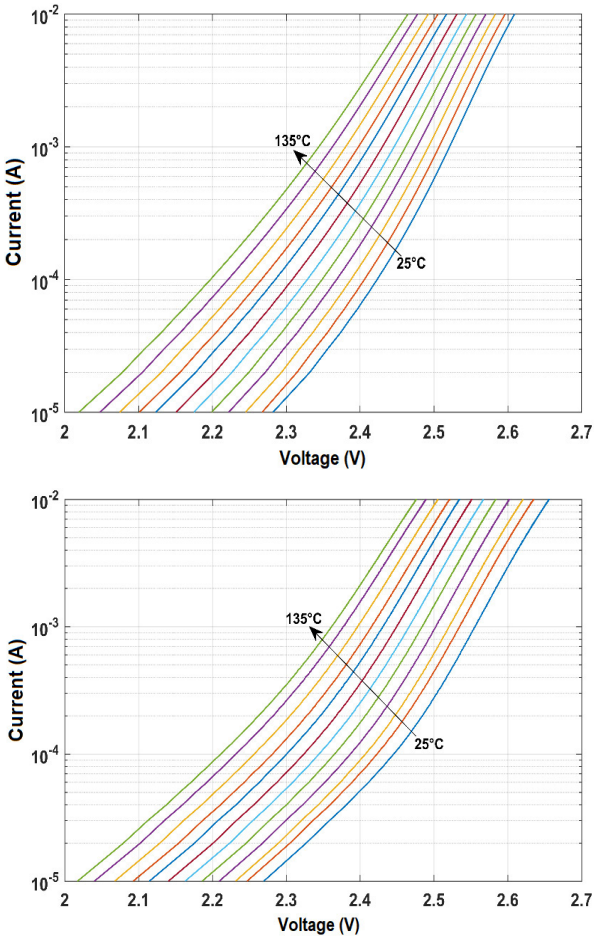


**FIGURE 1.** Typical current-voltage characteristics of LED-A (top graph) and LED-B (bottom graph) types measured between 25 and 135 °C, in steps of 10° C.

The coefficient of determination $R^2$ was calculated to evaluate the agreement between the experimental data $V_F$ *vs.* $T$ at each probe current and their best linear fit, $f_L(T)$. In particular, $R^2$ allows quantifying the sensor linearity goodness when the experimental data are fitted with a linear model. It was calculated by the following formula [41]:

$$R^2 = 1 - \frac{\sum_{i=1}^{n} \left(V_{F,i} - f_{L,i}\right)^2}{\sum_{i=1}^{n} \left(V_{F,i} - \bar{V}_F\right)^2}, \tag{5}$$

where $n$ is the number of the experimental points, $V_{F,i}$ and $f_{L,i}$ are the values provided by the actual measure and by the best linear fit model, respectively, at the $i$-th temperature, and $\bar{V}_F$ is the average of all measurements.

Another important parameter characterizing the goodness of the linear approximation of a temperature sensor is the temperature error *rmse*(°C), between $f_L(T)$ and the experimental data, evaluated as:

$$rmse = \frac{rmse\_V_F}{S} = \frac{\sqrt{\frac{\sum_{i=1}^{n} \left(V_{F,i} - f_{L,i}\right)^2}{n}}}{S}, \tag{6}$$

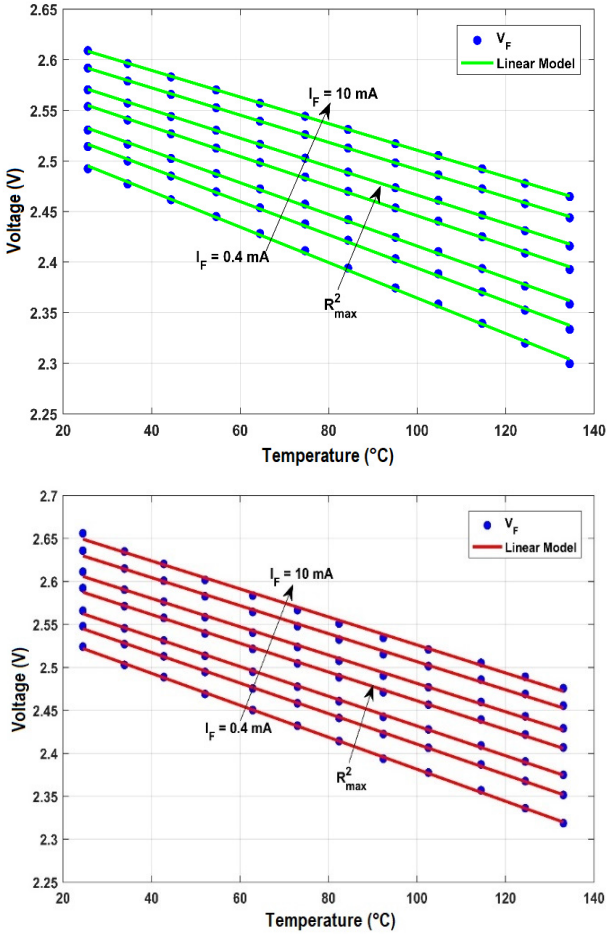


**FIGURE 2.** Measured (dots) forward voltage $V_F$ versus temperature at seven probe currents $I_F$ (0.4 mA, 0.8 mA, 1.3 mA, 2.4 mA, 3.8 mA, 6.6 mA and 10 mA), for the LED-A (top graph) and LED-B (bottom graph) of Fig. 1. Experimental data are fitted with their best calculated linear models (lines). In both graphs, the $R^2_{max}$ arrow indicate the curve with the highest linearity.

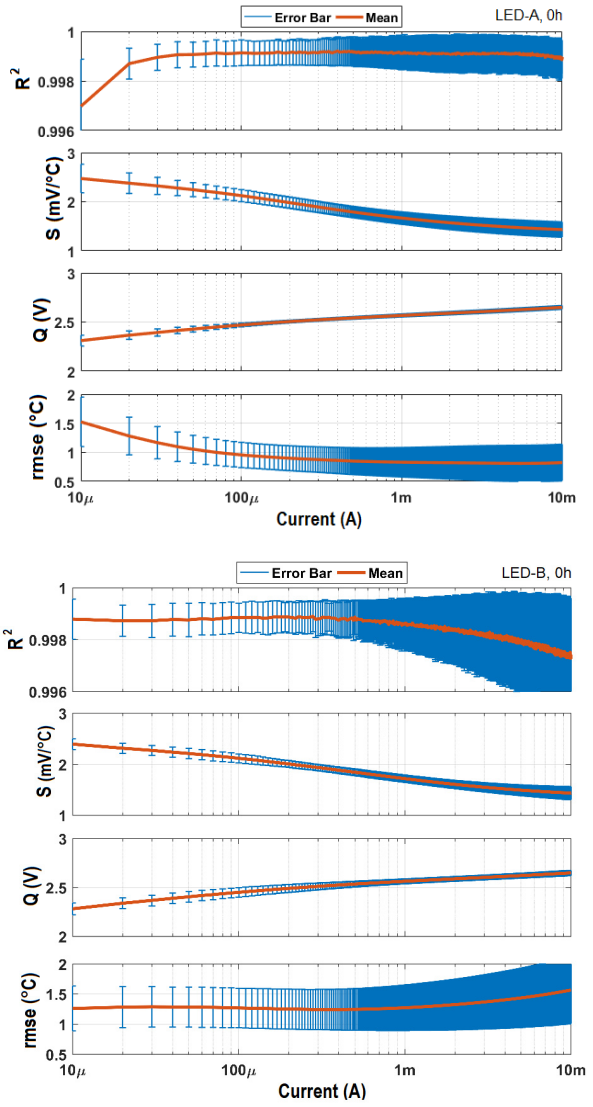


**FIGURE 3.** Experimental mean values of $R^2$, sensitivity $S$, intercept $Q$, and root mean square error *rmse* of the characterized LED-A (top) and LED-B (bottom) samples. Six new samples were characterized for each LED type.

where $rmse\_V_F$(V) is the root mean square error of the diode voltage drop, and $S$ (V/°C) is the sensor sensitivity, obtained from the slope of $f_L(T)$. In the temperature range between 25 °C and 135 °C, both samples show a high degree of linearity, as predicated by (4), with an $R^2 > 0.999$ in a wide range of currents (Fig. 2). In particular, the highest linearity with the lowest error is obtained at $I_F \approx 0.4$ mA for LED-A ($R^2 = 0.9998$), while for LED-B the best probe current is $I_F \approx 0.5$ mA ($R^2 = 0.9997$).

### B. EVALUATION OF THE AVERAGE SENSING PARAMETERS FOR EACH LED TYPE

After showing the two LEDs' ability to be used as highly linear temperature sensors, the average characteristics of each LED type was determined on more samples by proceeding with a long campaign of measurements. Six new devices of each type were in fact characterized with the same procedure described above.

The experimentally determined mean values of $S$, $R^2$ and *rmse*, as they were defined above, are shown in Fig. 3 both for LED-A and LED-B devices, together with the corresponding error bars. The reported values were calculated as the arithmetic mean of the experimental values measured on all samples of each LED type, at each probe current. The plots also include the parameter $Q$ (V), which represents the intercept with the $x$-axis of the linear best fits of Fig. 2, so that the $S$ and $Q$ values provided in Fig. 3 allow to express, at any desired probe current, the correct $V_F$ vs. $T$ relationship in the form:

$$V_F = -S \cdot T + Q, \tag{7}$$

and therefore calculate the actual junction temperature by simply measuring the forward voltage drop, with an approximation given by the *rmse* provided in the same figure.

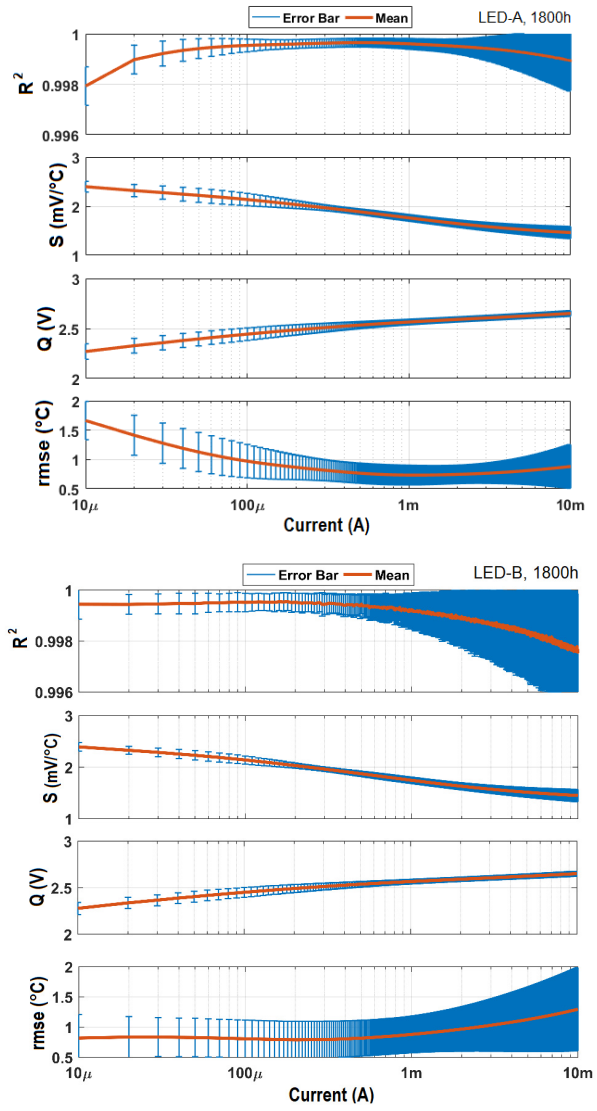


**FIGURE 4.** Experimental mean values and error bars of $R^2$, sensitivity $S$, intercept $Q$, and root mean square error *rmse* of the characterized LED-A (top) and LED-B (bottom) samples of Fig. 3 after 1800 h of operation at $I_F = 500$ mA and a temperature of 80 °C.

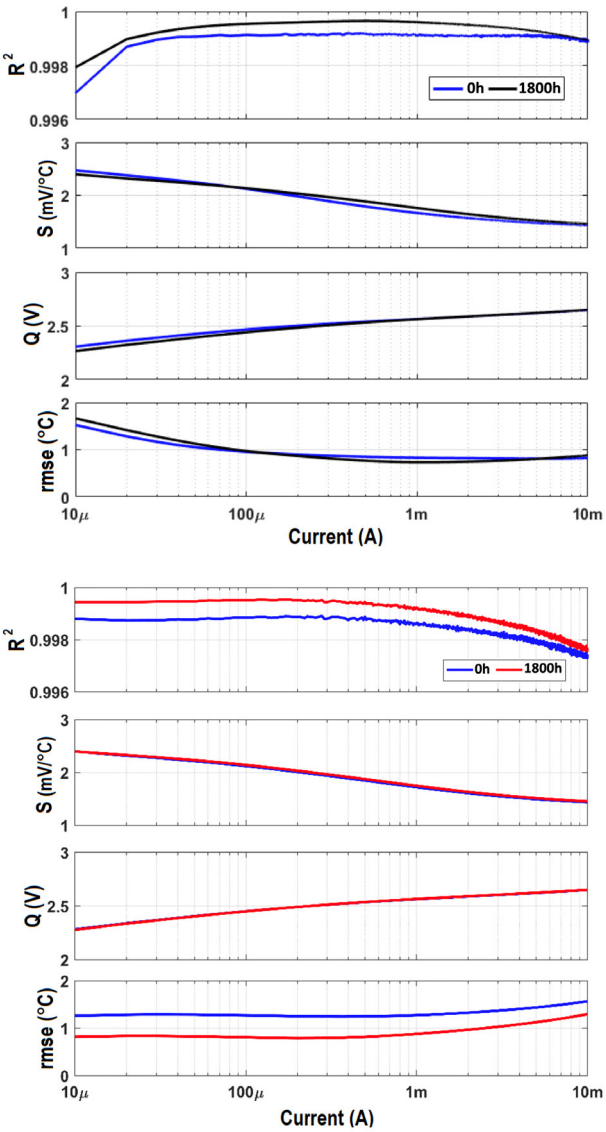


**FIGURE 5.** Comparison between the experimental mean values of $R^2$, sensitivity $S$, intercept $Q$, and root mean square error *rmse* of the characterized LED-A (top) and LED-B (bottom) samples of Fig. 3 at 0 h and after 1800 h of operation at $I_F = 500$ mA and a temperature of 80 °C.

### C. THERMAL STABILITY

To test the sensor stability over time, measurements were repeated after 600, 900, 1200 and 1800 hours of operation at a bias current of 500 mA and a temperature of 80 °C. After each time period, the LEDs were again fully characterized between room temperature and 135 °C, in the whole current range (10 $\mu$A to 10 mA).

The experimentally determined values of $S$, $Q$, $R^2$ and *rmse* after 1800 h stress are shown in Fig. 4. The curves do not show an evident deviation from those of new devices (Fig. 3). This is even more clear in Fig. 5, where the same average parameters are directly compared. It also shows that the sensor linearity and error are stable, or even improve with time.

For comparison purposes, the sensing parameters of LED-A, averaged over the six samples, are detailed in Table 2 at several probe currents and after a 1800 h stress. At $I_F = 0.6$ mA this LED type shows the best linearity ($R^2 = 0.99964$) and the lowest error ($rmse = 0.75$ °C). A list of the same characteristic values is reported in Table 3 for LED-B type, which shows the best performances at a probe current of 0.3 mA. It is worthwhile noting that an error of the order of 1 °C can be considered small enough for LED temperature monitoring in lighting applications, also considering that we are directly measuring $T_J$, and not a somehow correlated temperature. Given the small *rmse*, we can expect that these values, obtained on a limited set of devices, would be confirmed on larger sample sets, at least as long as high quality LEDs are concerned.

In order to derive the temperature from the forward voltage appearing on the device, it is highly desirable that the linear

**TABLE 1. Table of symbols and units.**

| Symbol | Units | Quantity |
|---|---|---|
| $E_g$ | eV | Energy gap |
| $f_L(T)$ | V | Best linear approximation of experimental $V_F$ vs. $T$ (at fixed $I_F$) |
| $f_{L,i}$ | V | $V_F$ at the $i$-th temperature as calculated by the linear model |
| $I_F$ | A | LED bias current |
| $I_{F,set}$ | A | Desired probe current for LED |
| $I_S$ | A | reverse saturation current |
| $P_D$ | W | Power dissipated on LED |
| $q$ | eV | Electron charge |
| $Q$ | V | x-axis intercept of the best linear approximation $f_L(T)$ |
| $R^2$ | - | Coefficient of determination of the linear regression (5) |
| $R_S$ | Ω | Internal stray resistance of LED |
| $R\Theta$ | K/W | Thermal resistance of LED (junction to environment) |
| $rmse$ | °C | Root mean square error of $T$ |
| $rmse\_VF$ | V | Root mean square error of measured $V_F$ |
| $S$ | V/°C | LED sensitivity, $dV_F/dT_J$ |
| $T$ | °C | Device temperature in °C |
| $T_A$ | K | Absolute temperature |
| $T_J$ | °C | LED junction temperature |
| $T_X$ | °C | Environment temperature |
| $V_F$ | V | Forward voltage drop at LED terminals |
| $V_{F,i}$ | V | Experimental $V_F$ at the $i$-th temperature |
| $\bar{V}_F$ | V | Average $V_F$ |
| $V_{F,n}$ | V | Voltage drop across a series of n LEDs |
| $\eta$ | - | Current ideality factor |

**TABLE 2. Sensing parameters of LED-A calculated after a stress of 1800h at 500mA and 80°C.**

| $I_F$ (mA) | $R^2$ | $S$ (mV/°C) | $Q$ (mV) | $rmse$ (°C) |
|---|---|---|---|---|
| 0.1 | 0.99954 | 2.134 | 2.444 | 0.97 |
| 0.6 | 0.99964 | 1.835 | 2.547 | 0.75 |
| 2.0 | 0.99949 | 1.645 | 2.591 | 0.76 |
| 5.0 | 0.99928 | 1.525 | 2.624 | 0.80 |
| 10.0 | 0.99894 | 1.462 | 2.651 | 0.88 |

**TABLE 3. Sensing parameters of LED-B calculated after a stress of 1800h at 500mA and 80°C.**

| $I_F$ (mA) | $R^2$ | $S$ (mV/°C) | $Q$ (mV) | $rmse$ (°C) |
|---|---|---|---|---|
| 0.1 | 0.99950 | 2.139 | 2.449 | 0.80 |
| 0.3 | 0.99951 | 1.975 | 2.508 | 0.79 |
| 2.0 | 0.99895 | 1.631 | 2.590 | 0.96 |
| 5.0 | 0.99833 | 1.513 | 2.623 | 1.12 |
| 10.0 | 0.99764 | 1.451 | 2.649 | 1.29 |

relationship (7) remains stable over time, once a proper probe current and the associate $S$ and $Q$ parameters are chosen. The stability of the LED types considered in this work is highlighted in Fig. 6, cumulatively showing the experimental points $V_F$ vs. $T$ at a probe current of 0.5 mA, of new devices and at the end of each stress time periods. The plots

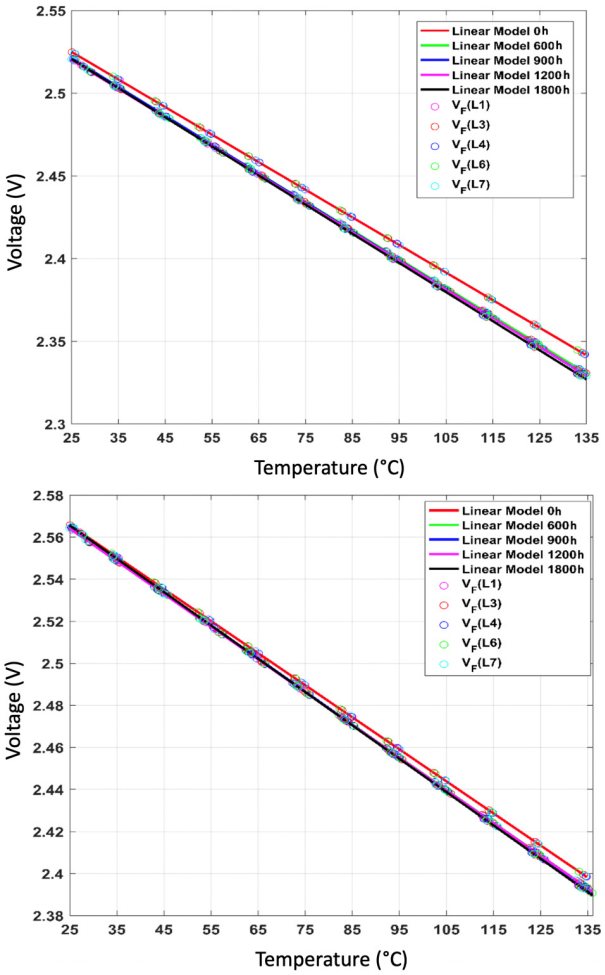


**FIGURE 6. Average measured forward voltage $V_F$ (circles) versus temperature at a probe current $I_F = 0.5$ mA for LED-A (top graph) and LED-B (bottom graph) devices. Experimental data are fitted with their best calculated linear models (lines).**

demonstrate that the sensing characteristics of the devices stabilize after a few hundred hours of operation.

The high linearity and small $rmse$ shown by these devices allow to assume that this technique could be also applied to a series-connected LEDs, as frequently used in luminaires. In this case, the input-output characteristics for n-series-connected LEDs can be described by the following equation:

$$V_{F,n} = n \cdot (-S \cdot T + Q), \tag{8}$$

where $V_{F,n}$ is the overall voltage appearing across the series, $n$ is the number of LEDs, and $S$ and $Q$ are respectively the average sensitivity and intercept of the y-axis calculated for the LED type. Of course, in this case $T$ represents the average value among the different junction temperatures.

## IV. LED JUNCTION TEMPERATURE MEASUREMENT CIRCUIT

### A. CIRCUIT

A practical circuit performing the LED junction temperature measurement is shown in Fig. 7. The measurement routine is

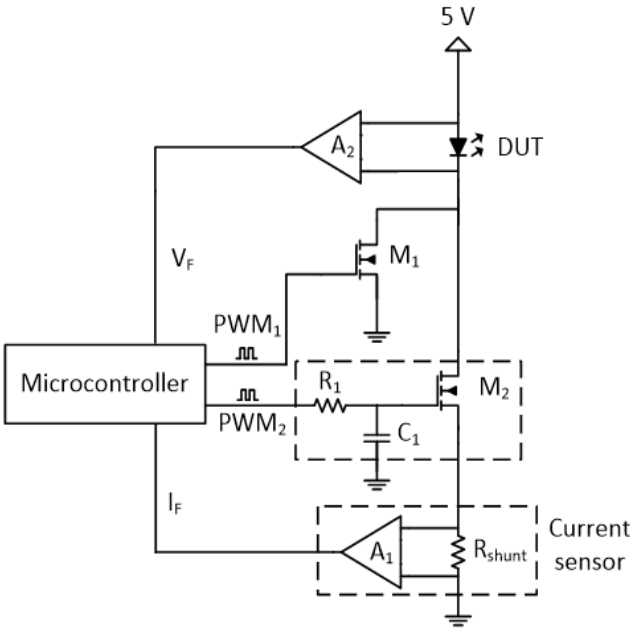


**FIGURE 7.** LED temperature measurement circuit.

basically governed by an ST NUCLEO-F401RE board [42] mounting an STM32F401RE microcontroller. A firmware was developed to generate two pulse-width modulation signals ($PWM_1$ and $PWM_2$) with a frequency of 5 kHz. $PWM_1$ is used to control the gate of MOSFET $M_1$ that forward biases the LED during normal operation (LED fully on). In this phase $M_2$ is off, the current sensor $A_1$ (Texas Instrument INA285 [43]), with a 1 Ω shunt-resistor, measures the current through the LED, while the duty cycle of $PWM_1$ is continuously adjusted to hold this current nearby the desired value, *e.g.* $I_F = 500$ mA.

At the start of the temperature measurement routine, $M_1$ is turned off (duty cycle of $PWM_1$ set to zero), while $PWM_2$ drives the LED by biasing the gate of $M_2$ through a low pass filter ($R_1 = 2\,k\Omega$, $C_1 = 5\,\mu F$). During this phase, which lasts less than 10 ms, the duty cycle of $PWM_2$ increases progressively in order to bias the LED with a current ramp comprised in a given range, *e.g.* 0.1 mA $< I_F <$ 1 mA. At each sampling time of the analog-digital converter, the actual value of the $I_F$ flowing through the device is measured through $A_1$, while the corresponding voltages $V_F$ across the LED is amplified through an instrumentation amplifier $A_2$ (Analog Devices LT1167 [44]).

The implemented firmware therefore calculates the junction temperature through the following steps:

1) while the LED is on, at some time $PWM_1$ is turned off and a few milliseconds long $PWM_2$ sequence, with a growing duty-cycle, is applied to $M_2$;
2) the values of the actual flowing currents $I_F$ and of the corresponding voltages $V_F$ across the DUT are measured through $A_1$ and $A_2$ of Fig. 7 and sampled by the microcontroller with the integrated 12-bit analog-digital converter;
3) the microcontroller then selects the $(V_F, I_F)$ couple corresponding to a previously identified probe current $I_{F,set}$. If no measure is found at $I_{F,set}$, the procedure is repeated a few hundred milliseconds later;
4) the junction temperature $T_J$ is calculated using (7), for which the values of sensitivity $S$ and of the intercepts with the y axis of the output characteristic $Q$ were previously stored in the microcontroller.

The steps used for temperature calculation are summarized in the flowchart of Fig. 8. This technique avoids the use of a temperature compensated current source to drive the LED at the desired probe current during the measurement routine, but can take seconds before the sought $(V_F, I_{F,set})$ couple is spotted. A more complex closed loop control circuit might be alternatively adopted, imposing the desired probe current $I_{F,set}$. The short acquisition routine (less than 10 ms) is not perceived by the human eye, especially in those cases where it can be randomly applied to LEDs that are parts of a matrix.

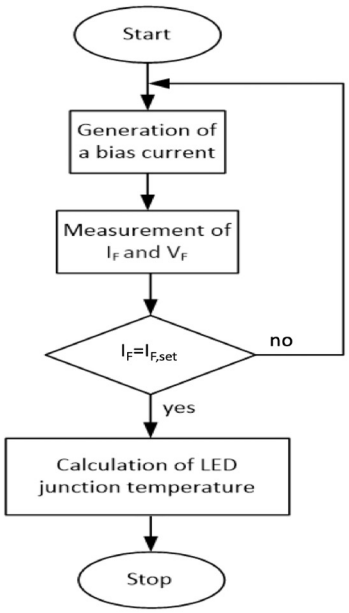


**FIGURE 8.** Flowchart of the LED junction temperature measuring sequence.

As an example of application, the conceived system could detect when the calculated junction temperature is above a threshold value (*e.g.* 95 °C), triggering the necessary countermeasures. A monitoring device, or the system itself, could *e.g.* issue a request for a temperature reduction action that can be started by reducing the bias current normally flowing through the LED.

### B. EXPERIMENTAL RESULTS

In order to evaluate the accuracy of LEDs junction temperature measurement method and circuit, an analysis was carried out by placing five LED-A samples in the oven and gradually heating them up to known and stable temperatures. To prevent self-heating, measurements were performed with the LED

turned-off, by setting $PWM_1$ to zero. The measurements were carried out from room temperature up to the maximum value of 135 °C. Each measurement was performed only after verifying that the oven temperature had stabilized for a few minutes, so that also the LED junction had itself reached the thermal equilibrium with the oven. Also in this case, the actual oven temperature, and therefore the LED junction temperature, was monitored through a PT100 sensor with an accuracy of 0.2 °C, placed on the PCB very close to the DUT. The junction temperature values calculated through the circuit were then compared with the PT100 temperature.

At each temperature, four consecutive measurements were made, and for each measurement, the error was extracted. In Fig. 9, the experimental data for the five characterized LED-A devices are shown. The corresponding mean error is 1.41 °C. For temperatures above 95 °C, which might be considered as a safety threshold to avoid LED damaging, the error is always lower than 2.1 °C. In spite of the several error sources contributing to this error, including sensor accuracy, measured current and voltage accuracy, and noise, the overall accuracy still appears suitable for practical applications, as the true junction temperature is obtained in this case.

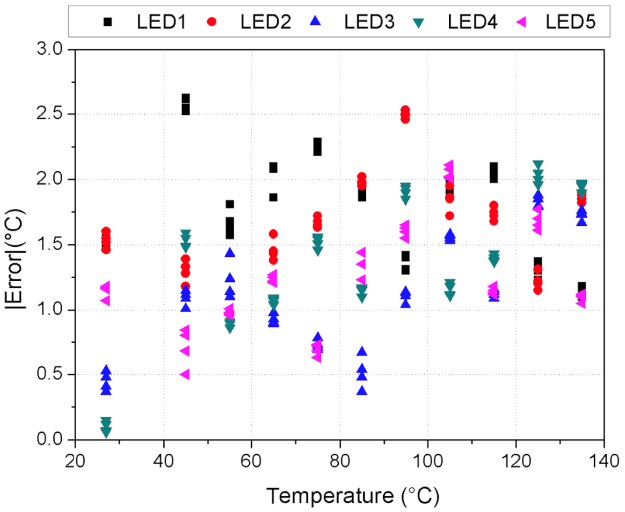


**FIGURE 9. Temperature error for five LED-A type devices, using the microcontroller-based acquisition circuit. On the horizontal axis the temperature calculated by the proposed circuit is reported.**

## V. CONCLUSION

The well-known dependence between temperature and the voltage appearing at diode terminals at a fixed current was fully characterized in off-the-shelf power light emitting diodes from two manufacturers, with the aim of using them as sensors of their own junction temperature, $T_J$. The experimental measurements were performed on twelve commercial devices at one thousand different probe currents, from 10 $\mu$A to 10 mA, and the linear fitting parameters $S$ (slope) and $Q$ (intercept) were calculated for each current, valid in the temperature range from 25 °C to 135 °C, together with the coefficient of determination $R^2$ and the root mean square error of $T$ introduced by the linear approximation. The devices showed both a high degree of linearity, with a value of $R^2$ higher than 0.9999 in a wide current range, and a good sensitivity ($S \approx 2$ mV/°C). The error was calculated to be lower than 1 °C. It has been observed that, after the application of a few hundred hours of current-temperature stress, the LED $V_F$ vs. $T$ characteristics stabilize.

A microcontroller-based circuit was designed and realized for the real-time monitoring of an LED temperature during its normal operation, demonstrating that a precise and stable current source is not necessary for measurements and that the readout technique provides good precision in spite of the simplicity of its implementation. Through experimental tests, it was in fact possible to verify the correctness of measurements and the reliability of the implemented method. It can be suggested that LED manufacturers should provide $S$ and $Q$ to allow an easy determination of their LED $T_J$ through a simple current-voltage measurement.

## ACKNOWLEDGMENT

The authors would like to thank L. Greco, P. Iannì, E. Mallemace, and S. Polimeni of the Mediterranea University of Reggio Calabria, Italy, for their help with the experimental measurements. PAC Calabria 2014-2020 Asse Prioritario 12, Azione 10.5.12, is also gratefully acknowledged by D. Iero.

## REFERENCES

[1] M. Meneghini, A. Tazzoli, G. Mura, G. Meneghesso, and E. Zanoni, "A review on the physical mechanisms that limit the reliability of GaN-based LEDs," *IEEE Trans. Electron Devices*, vol. 57, no. 1, pp. 108–118, Jan. 2010.

[2] J. Hu, L. Yang, and M. W. Shin, "Electrical, optical and thermal degradation of high power GaN/InGaN light-emitting diodes," *J. Phys. D, Appl. Phys.*, vol. 41, no. 3, Jan. 2008, Art. no. 035107.

[3] F.-K. Wang and Y.-C. Lu, "Useful lifetime analysis for high-power white LEDs," *Microelectron. Rel.*, vol. 54, nos. 6–7, pp. 1307–1315, Jun. 2014.

[4] N. Narendran, Y. Gu, J. P. Freyssinier, H. Yu, and L. Deng, "Solid-state lighting: Failure analysis of white LEDs," *J. Cryst. Growth*, vol. 268, nos. 3–4, pp. 449–456, Aug. 2004.

[5] M. Dal Lago, M. Meneghini, N. Trivellin, G. Mura, M. Vanzi, G. Meneghesso, and E. Zanoni, "Phosphors for LED-based light sources: Thermal properties and reliability issues," *Microelectron. Rel.*, vol. 52, nos. 9–10, pp. 2164–2167, Sep. 2012.

[6] M.-H. Kim, M. F. Schubert, Q. Dai, J. K. Kim, E. F. Schubert, J. Piprek, and Y. Park, "Origin of efficiency droop in GaN-based light-emitting diodes," *Appl. Phys. Lett.*, vol. 91, no. 18, 2007, Art. no. 183507.

[7] N. Narendran and Y. Gu, "Life of LED-based white light sources," *J. Display Technol.*, vol. 1, no. 1, pp. 167–171, Sep. 2005.

[8] A. Poppe, G. Molnar, and T. Temesvolgyi, "Temperature dependent thermal resistance in power LED assemblies and a way to cope with it," in *Proc. 26th Annu. IEEE Semicond. Therm. Meas. Manage. Symp. (SEMI-THERM)*, Feb. 2010, pp. 283–288.

[9] M. Meneghini, M. D. Lago, N. Trivellin, G. Meneghesso, and E. Zanoni, "Degradation mechanisms of high-power LEDs for lighting applications: An overview," *IEEE Trans. Ind. Appl.*, vol. 50, no. 1, pp. 78–85, Jan./Feb. 2014.

[10] M. Meneghini, L. Trevisanello, C. Sanna, G. Mura, M. Vanzi, G. Meneghesso, and E. Zanoni, "High temperature electro-optical degradation of InGaN/GaN HBLEDs," *Microelectron. Rel.*, vol. 47, nos. 9–11, pp. 1625–1629, Sep. 2007.

[11] J. Huang, D. S. Golubovic, S. Koh, D. Yang, X. Li, X. J. Fan, and G. Q. Zhang, "Degradation mechanisms of mid-power white-light LEDs under high-Temperature–Humidity conditions," *IEEE Trans. Device Mater. Rel.*, vol. 15, no. 2, pp. 220–228, Jun. 2015.

[12] F.-K. Wang and T.-P. Chu, "Lifetime predictions of LED-based light bars by accelerated degradation test," *Microelectron. Rel.*, vol. 52, no. 7, pp. 1332–1336, Jul. 2012.

[13] A. Christensen and S. Graham, "Thermal effects in packaging high power light emitting diode arrays," *Appl. Therm. Eng.*, vol. 29, nos. 2–3, pp. 364–371, Feb. 2009.

[14] Z. Vaitonis, P. Vitta, and A. Žukauskas, "Measurement of the junction temperature in high-power light-emitting diodes from the high-energy wing of the electroluminescence band," *J. Appl. Phys.*, vol. 103, no. 9, May 2008, Art. no. 093110.

[15] Y. Wang, H. Xu, S. Alur, A. Cheng, M. Park, S. Sakhawat, N. Arindra, O. Akpa, S. Akavaram, and K. Das, "Determination of junction temperature of GaN-based light emitting diodes by electroluminescence and micro-Raman spectroscopy," *Proc. CS MANTECH Conf.*, 2009, pp. 1–3.

[16] M. Horiuchi, Y. Yamagata, S.-I. Tsutsumi, K. Tomita, and Y. Manabe, "Development of junction temperature estimation system for light-emitting LED using pulsed-laser Raman scattering," *J. Solid State Lighting*, vol. 2, no. 1, p. 7, Jul. 2015.

[17] A. Keppens, W. R. Ryckaert, G. Deconinck, and P. Hanselaer, "Modeling high power light-emitting diode spectra and their variation with junction temperature," *J. Appl. Phys.*, vol. 108, no. 4, Aug. 2010, Art. no. 043104.

[18] C. C. Lee and J. Park, "Temperature measurement of visible light-emitting diodes using nematic liquid crystal thermography with laser illumination," *IEEE Photon. Technol. Lett.*, vol. 16, no. 7, pp. 1706–1708, Jul. 2004.

[19] Z. Zha, H. Wong, and Y. Han, "An LED driver with thermal control function," in *Proc. 12th IEEE Int. Conf. Solid-State Integr. Circuit Technol. (ICSICT)*, Oct. 2014, pp. 1–3.

[20] Q. Chen, X. Luo, S. Zhou, and S. Liu, "Dynamic junction temperature measurement for high power light emitting diodes," *Rev. Sci. Instrum.*, vol. 82, no. 8, Aug. 2011, Art. no. 084904.

[21] *Overview of Methodologies for the Thermal Measurement of Single- and Multi-Chip, Single- and Multi-PN-Junction Light-Emitting Diodes (LEDs)*, dcoument JESD51-50, JEDEC Solid State Technology Association, Arlington, VA, USA, 2012.

[22] *Implementation of the Electrical Test Method for the Measurement of Real Thermal Resistance and Impendance of Light-Emitting Diodes With Exposed Cooling*, document JESD51-51, JEDEC Solid State Technology Association, Arlington, VA, USA, 2012.

[23] B. Wu, S. Lin, T.-M. Shih, Y. Gao, Y. Lu, L. Zhu, G. Chen, and Z. Chen, "Junction-temperature determination in InGaN light-emitting diodes using reverse current method," *IEEE Trans. Electron Devices*, vol. 60, no. 1, pp. 241–245, Jan. 2013.

[24] Y. Xi and E. F. Schubert, "Junction-temperature measurement in GaN ultraviolet light-emitting diodes using diode forward voltage method," *Appl. Phys. Lett.*, vol. 85, no. 12, pp. 2163–2165, Sep. 2004.

[25] A. Keppens, W. R. Ryckaert, G. Deconinck, and P. Hanselaer, "High power light-emitting diode junction temperature determination from current-voltage characteristics," *J. Appl. Phys.*, vol. 104, no. 9, Nov. 2008, Art. no. 093104.

[26] Y. B. Acharya and P. D. Vyavahare, "Study on the temperature sensing capability of a light-emitting diode," *Rev. Sci. Instrum.*, vol. 68, no. 12, pp. 4465–4467, Dec. 1997.

[27] F. D. R. Abbing and M. A. P. Pertijs, "Light-emitting diode junction-temperature sensing using differential voltage/current measurements," in *Proc. IEEE SENSORS*, Oct. 2011, pp. 861–864.

[28] S. Rao, G. Pangallo, F. Pezzimenti, and F. G. D. Corte, "High-performance temperature sensor based on 4H-SiC Schottky diodes," *IEEE Electron Device Lett.*, vol. 36, no. 7, pp. 720–722, Jul. 2015.

[29] S. Rao, G. Pangallo, and F. G. D. Corte, "4H-SiC p-i-n diode as highly linear temperature sensor," *IEEE Trans. Electron Devices*, vol. 63, no. 1, pp. 414–418, Jan. 2016.

[30] L. Di Benedetto, G. D. Licciardo, S. Rao, G. Pangallo, F. G. D. Corte, and A. Rubino, "$V_2O_5$/4H-SiC Schottky diode temperature sensor: Experiments and model," *IEEE Trans. Electron Devices*, vol. 65, no. 2, pp. 687–694, Feb. 2018.

[31] S. Rao, L. Di Benedetto, G. Pangallo, A. Rubino, S. Bellone, and F. G. D. Corte, "85–440 K temperature sensor based on a 4H-SiC Schottky diode," *IEEE Sensors J.*, vol. 16, no. 17, pp. 6537–6542, Jul. 2016.

[32] C. D. Matthus, T. Erlbacher, A. Hess, A. J. Bauer, and L. Frey, "Advanced 4H-SiC pin diode as highly sensitive high-temperature sensor up to 460 °C," *IEEE Trans. Electron Devices*, vol. 64, no. 8, pp. 3399–3404, Aug. 2017.

[33] N. Zhang, C.-M. Lin, D. G. Senesky, and A. P. Pisano, "Temperature sensor based on 4H-silicon carbide pn diode operational from 20 °C to 600 °C," *Appl. Phys. Lett.*, vol. 104, no. 7, Feb. 2014, Art. no. 073504.

[34] S. Rao, G. Pangallo, and F. D. Corte, "Integrated amorphous silicon p-i-n temperature sensor for CMOS photonics," *Sensors*, vol. 16, no. 1, p. 67, Jan. 2016.

[35] S. Santra, P. K. Guha, S. Z. Ali, I. Haneef, and F. Udrea, "Silicon on insulator diode temperature sensor—A detailed analysis for ultra-high temperature operation," *IEEE Sensors J.*, vol. 10, no. 5, pp. 997–1003, May 2010.

[36] (2018). *OSRAM Opto Semiconductors LUW CQAR-NPNR-HPJR-1-700 Datasheet*. [Online]. Available: https://dammedia.osram.info/media/resource/hires/osram-dam-5537536/LUW%20CQAR%20(streetwhite)_EN.pdf

[37] *NICHIA NVSW319AT-6570 Datasheet*. Accessed: Jan. 2, 2020. [Online]. Available: https://docs-emea.rs-online.com/webdocs/15c3/0900766b815c3e42.pdf

[38] G. Pangallo, R. Carotenuto, D. Iero, E. D. Mallemace, M. Merenda, S. Rao, and F. G. D. Corte, "A direct junction temperature measurement technique for power LEDs," in *Proc. IEEE 9th Int. Workshop Appl. Meas. Power Syst. (AMPS)*, Sep. 2018, pp. 26–28.

[39] F. Galli. (2014). *Galli-Stufe-Ovens-2100*. [Online]. Available: https://www.herascientific.com/wp-content/uploads/2014/03/Galli-Stufe-Ovens-2100.pdf

[40] Agilent Tecnologies. (2000). *Agilent 4155B/4156B User's Guide*. [Online]. Available: http://eecs.oregonstate.edu/matdev/man/Agilent4155C_4156C_Users_Guide_Vol1.pdf

[41] N. J. D. Nagelkerke, "A note on a general definition of the coefficient of determination," *Biometrika*, vol. 78, no. 3, pp. 691–692, Sep. 1991.

[42] STMicroelectronics. *NUCLEO-F401RE board User Manual*. Accessed: Jan. 2, 2020. [Online]. Available: https://www.st.com/content/ccc/resource/technical/document/user_manual/98/2e/fa/4b/e0/82/43/b7/DM00105823.pdf/files/DM00105823.pdf/jcr:content/translations/en.DM00105823.pdf

[43] Texas Instrument. (2015). *INA28x Datasheet*. [Online]. Available: http://www.ti.com/lit/ds/symlink/ina283-q1.pdf

[44] Analog Devices. *LT1167 Datasheet*. Accessed: Jan. 2, 2020. [Online]. Available: https://www.analog.com/media/en/technical-documentation/data-sheets/1167fc.pdf

**FRANCESCO G. DELLA CORTE** (Senior Member, IEEE) received the Laurea degree in electronic engineering from the University of Napoli, Naples, Italy, in 1988. He is currently a Full Professor of electronics with the Mediterranea University of Reggio Calabria, Reggio Calabria, Italy. His current research interests include wide bandgap semiconductor device modeling for high temperature and high power applications, silicon photonics, and wireless smart sensors.

**GIOVANNI PANGALLO** was born in Reggio Calabria, Italy, in 1986. He received the B.E. and M.E. degrees in electronic engineering and the Ph.D. degree in information engineering from the Mediterranea University of Reggio Calabria, Italy, in 2010, 2013, and 2018, respectively. His current research interest includes power systems and sensors for hostile environments.

**RICCARDO CAROTENUTO** (Senior Member, IEEE) was born in Rome, Italy. He received the Dr.Sc. degree in electronic engineering and the Ph.D. degree from the Sapienza University of Rome, Rome, Italy. He is currently an Associate Professor of electronics with the Mediterranea University of Reggio Calabria, Reggio Calabria, Italy. His current research interests include indoor positioning, smart sensors, and ultrasound imaging.

**DEMETRIO IERO** received the master's degree in electronic engineering and the Ph.D. degree from the Mediterranea University of Reggio Calabria, Reggio Calabria, in 2010 and 2014, respectively. He is currently a temporary Research Associate with the DIIES Department, Mediterranea University of Reggio Calabria. His current research interests include power electronics and switching power loss measurement, microcontrollers, the Internet of Things, and RFID platforms.

**GIUSEPPE MARRA** was born in Reggio Calabria, Italy, in 1994. He received the B.Sc. degree in information engineering and the M.Sc. degree in electronic engineering from the Mediterranea University of Reggio Calabria, Reggio Calabria, in 2017 and 2019, respectively. His research interest is in the field of semiconductor temperature sensors.

**MASSIMO MERENDA** (Member, IEEE) received the B.S., M.S., and Ph.D. degrees in electronic engineering from the Mediterranea University of Reggio Calabria, Italy, in 2002, 2005, and 2009, respectively. From 2003 to 2005, he was a Fellow at IMM-CNR, Naples, Italy. Since December 2018, he has been an Assistant Professor with the DIIES Department, Mediterranea University of Reggio Calabria. He has authored more than 40 articles published on international journals and conferences proceedings and holds four patents. His research involved the design and development of application specific integrated circuits (ASIC), silicon sensors, embedded systems, and intelligent radiofrequency identifiers (smart-RFID).

**SANDRO RAO** (Member, IEEE) received the B.Sc., M.Sc., and Ph.D. degrees in electronics engineering from the Mediterranea University of Reggio Calabria, Reggio Calabria, Italy, in 2003, 2005, and 2008, respectively. He has been a Researcher of electronics with the Mediterranea University of Reggio Calabria, since 2012, where he is involved in the design, realization, and characterization of amorphous silicon CMOS compatible electro-optical modulators and on wide gap semiconductor devices.